*buildings*

MDPI

*Article*

# Simulation Study on the Effects of Relative Humidity (RH) on Long-Wave Radiative Heat Gain in Residential Buildings

**Jie Chen [1,2,3], Fei Xue [1,2,3], Xiaoxue Jin [1], Stephen Siu Yu Lau [3,4,*] and Yue Fan [1,2,3,*]**

[1] School of Architecture & Urban Planning, Shenzhen University, Shenzhen 518060, China; chenjie1122@szu.edu.cn (J.C.); xuefei@szu.edu.cn (F.X.); xiaoxie@szu.edu.cn (X.J.)
[2] State Key Laboratory of Subtropical Building and Urban Science, Shenzhen 518060, China
[3] Center for Human-Oriented Environment and Sustainable Design, Shenzhen University, Shenzhen 518060, China
[4] Faculty of Architecture, The University of Hong Kong, Hong Kong 999077, China
* Correspondence: ssylau@hku.hk (S.S.Y.L.); yfan@szu.edu.cn (Y.F.); Tel.: +86-199-2648-2922 (S.S.Y.L.)

**Abstract:** Long-wave radiation cooling plays a pivotal role in building thermal design. Utilizing a steady-state method to determine surface heat transfer coefficients across diverse climates can result in discrepancies between the designed and actual cooling performance of a building's envelope. To evaluate the influence of climate and surface emissivity on building heat transfer during summer, the numerical simulation method was employed to calculate the summer long-wave radiation for nine typical residential buildings across various climate regions. This study assesses the applicable meteorological conditions and distribution range of sky radiation technology. The findings indicate that buildings can effectively dissipate heat through sky radiation when the outdoor relative humidity is below 60% and the summer temperature difference exceeds 12 °C. Analysis of meteorological characteristics across different zones reveals a positive correlation between temperature deviations and sky radiative cooling potential, thereby identifying suitable climate zones for the implementation of sky radiative cooling technology.

**Keywords:** long-wave radiation cooling; numerical simulation; building load; climate adaptability



**Citation:** Chen, J.; Xue, F.; Jin, X.; Lau, S.S.Y.; Fan, Y. Simulation Study on the Effects of Relative Humidity (RH) on Long-Wave Radiative Heat Gain in Residential Buildings. *Buildings* **2024**, *14*, 3724. https://doi.org/10.3390/buildings14123724

Academic Editors: Paulo Santos and Apple L.S. Chan

Received: 15 October 2024
Revised: 10 November 2024
Accepted: 20 November 2024
Published: 22 November 2024



## 1. Introduction

Buildings account for 20% to 40% of global fossil energy consumption. With the rapid development of urbanization, the average energy intensity of urban residential households keeps increasing. In recent years, with the continuous improvement in the thermal insulation level of the building envelope, determining how to control the natural heat dissipation of buildings and the corresponding increase in air-conditioning energy consumption has caused a discussion on building envelope energy conservation [1–3]. Sky radiant cooling technology can improve the heat dissipation level of the building without consuming other energy sources and has good potential for building energy saving.

Long-wave radiation in the sky is a crucial component of Earth's energy budget and is vital for studies in atmospheric meteorology and climate modeling. The radiative cooling of building surfaces results from heat loss to the sky via long-wave heat transfer, an effective passive cooling technique [4]. Long-wave heat exchange is particularly pronounced at night when the building's outer surface temperature is significantly higher than the sky temperature. Therefore, the accurate measurement of sky long-wave radiation is essential for precise building energy predictions. On a clear night, a sky-facing surface emitting long-wave radiation through an atmospheric window in the 8–13 μm range of the electromagnetic spectrum can maintain temperatures below ambient levels. Besides the thermal optical properties of materials, radiative cooling is influenced by various environmental factors that determine atmospheric transmittance.

Although a pyrometer can be used directly, it is not a standard radiation collection device for meteorological observations [5–7], due to its higher cost compared to instruments that measure solar radiation and its limited availability at national stations. Measuring long-wave radiation from the sky also necessitates excluding long-wave radiation from surrounding obstacles such as buildings and trees. Directly measuring long-wave radiation with a radiometer will result in some overestimation. Various models for sky long-wave radiation have been developed for different climatic conditions, based on correlations between sky long-wave radiation and conventional meteorological parameters. These models are primarily categorized into empirical models, detailed models, and international standard models. Empirical models are highly localized as they are based on local meteorological data, whereas detailed models are more complex, incorporating atmospheric composition through detailed theoretical analysis. The International Standard Model offers a simple estimate of long-wave radiation, which can lead to significant errors. Most available models were developed under clear-sky conditions, and using these models under cloudy conditions introduces calculation errors. Radiative cooling performance may vary by geographic location. Li et al. proposed the radiative cooling resource map for the mainland United States [8]. Similarly, Zhu et al. and Chen et al. independently produced a comparable radiative cooling resource map for China [9,10].

The performance of radiative cooling is largely dependent on the transparency of the atmospheric window. Long-wave radiation emitted by the radiation cooler penetrates the clear sky through a highly transparent atmospheric window, with minimal scattering, attenuation, and absorption. However, atmospheric transparency is a dynamic property influenced by local meteorological conditions and can become obscured under wet, cloudy skies. Clouds play a crucial role in various aspects of the global energy budget system. A straightforward method for estimating long-wave (LW) radiation relies on the parametric modeling of meteorological variables routinely measured at the surface level, such as air temperature and relative humidity. These parametric models make specific assumptions about the vertical structure of the atmosphere, which are implicitly included in the model through local fitting coefficients [11–14]. To study the effects of humidity, cloud cover, and aerosol concentration, and to quantitatively reveal geographical differences in radiative cooling performance, Mengying Li proposed a new comprehensive model for estimating downward atmospheric long-wave (LW) radiation under various sky conditions, including sunny and multi-cloud scenarios. To explain the difference in clear-sky radiative cooling rates between nighttime and daytime, distinct Brunt-type models for nighttime and daytime were proposed. In all-sky conditions, cloud information is represented either by the cloud coverage fraction (CF) or by the cloud modification factor (CMF), which is only available during the day [15]. A new model is proposed for all-sky conditions (day and night, clear or cloudy skies). However, relative humidity is a meteorological data source that is easy to obtain compared to cloud amount data. In the study of building heat transfer through dynamic sky effective temperature, the calculation process is relatively complex, and the design indicators resulting from the research are difficult for architects to adopt in the early design stage.

The calculation method adopted in building thermal design standards ignores the impact of long-wave radiation, especially lacking in research on the sky radiative cooling performance of building heat transfer. During the architectural design process using sky long-wave radiation technology, there is a relative lack of research on climate suitability conditions and design indicators. The purpose of this study in calculating the range of relative humidity is to assess the relationship between climate factors and the potential application of radiative cooling technology. First, by establishing a dynamic sky radiation model and setting simulation calculation parameters, the long-wave radiation amount of the same building in different climate zones was calculated. Then, statistical analysis was performed on the radiation potential and relative humidity parameters. Finally, the applicable climate conditions and geographical range division for long-wave radiation cooling technology were obtained, which improved the accuracy of heat calculation for building

envelope structures and simplified the complex thermal calculation process required for the selection of sky radiation technology. Figure 1 provides an overview of this study.

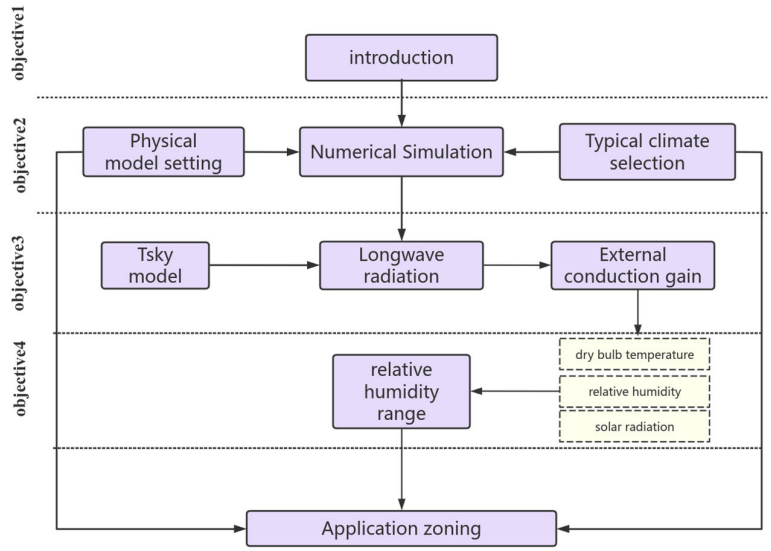


**Figure 1.** Schematic overview of workflow in the present study.

## 2. Research Methods

### *2.1. Calculation of Long-Wave Radiation*

This article only considers the one-dimensional steady-state heat transfer and periodic unsteady heat transfer problems of the main part of the building envelope. In the process of surface heat balance of the envelope structure, the heat gained by the wall is equal to the absorbed solar radiation heat minus the surface convective heat transfer, and then minus the radiative heat exchange with the ground and the long-wave radiation heat exchange with the atmosphere [16]. The essence of long-wave radiation is the radiation heat exchange between buildings and the sky, including the heat exchange between the ground and the surrounding building environment. The long-wave absorption rate is equal to the long-wave emissivity $\varepsilon_1$, the calculation is complicated, and the total absorption flux is the absorbed atmospheric component $\varepsilon_1 L_{sky(\beta)}$ and the absorbed ground component $\varepsilon_1 L_{g(\beta)}$.

$$F = \varepsilon_1 \sigma T_{eo}^4 \tag{1}$$

where F is radiative heat flux emitted by the surface ($W \cdot m^{-2}$); $\varepsilon_1$ is the long-wave surface emissivity; σ is the Stephen–Boltzmann constant ($5.6697 \times 10^{-8}$) ($W \cdot m^{-2} \cdot K^{-4}$); and $T_{eo}$ is absolute surface temperature (K).

The output long-wave flux is independent of the orientation of the emitting surface. The resulting slanted long-wave radiation energy exchange can be expressed as a net balance. The expression for the net long-wave radiation entering the surface of the envelope is

$$L(\beta) = \varepsilon_1 \left[ F_{s-sky} L_{sky(\beta)} + F_{s-g} L_{g(\beta)-} \sigma T_{eo}^4 \right] \tag{2}$$

where $L(\beta)$ is the long-wave radiation exchange ($W \cdot m^{-2}$); $L_{sky(\beta)}$ is the atmospheric long-wave radiation received directly from the sky ($W \cdot m^{-2}$); $L_{g(\beta)}$ is the long-wave radiation received from the ground ($W \cdot m^{-2}$); β is the surface inclination (°); $F_{s-g}$ is the angle coefficient of the outer surface facing the ground; and $F_{s-sky}$ is the angle coefficient of the outer surface facing the sky.

$$F_{s-g} = (1 - \cos\alpha)/\alpha \tag{3}$$

$$F_{s-sky} = (1 - \cos\alpha)/\alpha \tag{4}$$

For the special case of no occlusion on the horizontal plane, Equation (2) is simplified to

$$L = \varepsilon_1 \left( L_{sky} - \sigma T_{eo}^4 \right) \tag{5}$$

### 2.2. Sky Radiation Model

Various formulas have been proposed to estimate the long-wave radiation emitted from the atmosphere downwards and the ground upwards. Some models have been developed [17] for calculating the effective sky temperature on the horizontal plane under clear-sky conditions. The general empirical value is obtained by subtracting 6 K from the outdoor air temperature, which is the horizontal effective sky temperature [18].

Under clear-sky conditions, $\varepsilon$ can be modeled as a function of $T_a$ and/or vapor pressure, $e_a$, that is routinely measured in meteorological observatories and registered in automatic weather stations around the world [12,14,19–21].

$$L_{sky0} = \varepsilon_0(T_a, e_a)\sigma T_a^4 \tag{6}$$

where subscript "0" indicates clear-sky conditions. There exist numerous formulations to estimate $L_{sky0}$ from simple meteorological data.

On the other hand, under cloudy sky conditions, the long-wave radiation flux received at the surface is substantially modified. Liquid water and ice absorb and emit long-wave radiation more effectively than water in the vapor phase (most important atmospheric gas contributing to thermal radiation in the atmosphere), increasing the downward long-wave radiation. This is the reason why cloud cover plays an important role in estimating $L_{sky}$.

$$L_{sky} = \varepsilon_e(c, T_a, e_a)\sigma T_a^4 \tag{7}$$

where $\varepsilon_e$ is the effective emissivity of the atmosphere (under all-sky conditions) and c (dimensionless) is the cloud fraction, where it is more difficult to estimate downward long-wave radiation under cloudy sky conditions. Generally, effective emissivity is defined as $\varepsilon_e$ = f(c). $\varepsilon_0$ is a function of f(c) with c as input [22–27].

The procedure used here was based on the literature of Evangelisti et al. [17], and these detailed models formed the basis for the numerical simulation of long-wave radiation calculations. The daytime long-wave irradiance of the atmosphere on the horizontal plane can be estimated as

$$L_{sky} = \sigma T_a^4 \left[ 0.904 - \left( 0.304 - 0.061 \rho w^{1/2} \right) S_h - 0.005 \rho w^{1/2} \right] \tag{8}$$

where $L_{sky}$ is the daytime long-wave irradiance ($W \cdot m^{-2}$) on the horizontal plane; $\sigma$ is the Stephen–Boltzmann constant ($5.6697 \times 10^{-8}$) ($W \cdot m^{-2} \cdot K^{-4}$); $T_a$ is the absolute air temperature (K); $\rho w$ is the partial pressure of water vapor (hPa); and $S_h$ is the hourly insolation rate.

At night, $S_h$ is replaced with $[1 - (N_h/8)]$, where $N_h$ is hourly cloud cover. Since the values of $S_h$ are not stable during the first and last hours of the day, these two hours are considered nighttime hours. The daytime terrestrial long-wave upward flux is

$$L_g = \sigma \left[ 0.980 T_a + 0.037 \left( 1 - \rho_g \right) G_h \right]^4 \tag{9}$$

where $L_g$ is the long-wave radiation flux ($W \cdot m^{-2}$) on the horizontal plane; $T_a$ is the absolute air temperature (K); $\rho_g$ is the ground short-wave albedo; and $G_h$ is the hourly solar radiation ($W \cdot h \cdot m^{-2}$).

### 2.3. Selection of Typical Cities

The air-conditioning degree-days (CDD26) refers to the cooling demand index (qc), and the annual cooling energy consumption (Ec) of the comprehensive energy-saving index

limit for buildings is determined based on the cooling degree days (CDD26) of the location of the building. Its value is the number of days in a year when the daily average outdoor temperature is above 26 °C, multiplied by the degrees above 26 °C for each day, and then the sum of these products is accumulated. An indicator that represents the duration and degree of heat in a region was used as the standard and was divided into three grades according to the cooling demand. The representative cities and climate zones were selected, as shown in Table 1 [28]. The hottest period was from 26 May to 22 September (Table 2) [29], and the relatively concentrated cooling period from 25 June to 25 August was selected as the summer research period.

**Table 1.** Refrigeration requirement classification (GB50176-2016 [28]).

| Cooling Level | Representative City | CDD26 (°C·d) Degree Days for Air Conditioning | Thermal Partition |
|---|---|---|---|
| level 1 | Turpan | 579 | Cold regions |
| | East | 530 | Hot summer and warm winter area |
| | Haikou | 427 | Hot summer and warm winter area |
| level 2 | Guangzhou | 313 | Hot summer and cold winter area |
| | Wuhan | 283 | Hot summer and cold winter area |
| | Chongqing | 217 | Hot summer and cold winter area |
| level 3 | Karamay | 196 | Frigid regions |
| | Xi'an | 153 | Cold regions |
| | Beijing | 94 | Cold regions |

**Table 2.** Typical city air-conditioning period in various climate regions (GB50176-2016 [28]).

| Climate Zone | Typical City | Air-Conditioning Period |
|---|---|---|
| Frigid regions | Harbin | None |
| Cold regions | Beijing | 20 June to 3 August |
| Hot summer and cold winter area | Changsha | 25 June to 23 August |
| Hot summer and warm winter area | Guangzhou | 26 May to 22 September |
| Temperate area | Kunming | None |

### *2.4. Simulation Settings*

A typical multi-story residential building is selected as the calculation object, as shown in Figure 2. The area of the envelope is 1350 $m^2$, with 15 m × 15 m × 18 m = 4050 $m^3$, and the surface area is 1305 $m^2$. Calculations and simulations are performed using IESVE numerical simulation software (www.iesve.com, accessed on 20 June 2023) using ApacheSim, ApacheHVAC, MacroFlo, ApacheCalc, and ASHRAE loads. Using the thermal model in the IESVE software, spatial modeling was conducted for building types and climate zones. The dynamic sky radiation model was selected to simulate energy, assess heat transfer in the building envelope, and provide detailed breakdown data of key driving factors. Weather data for outdoor boundary conditions use the standard CSWD weather file (https://energyplus.net/weather-region/, accessed on 10 April 2023). Developed for use in simulating building heating and air-conditioning loads and energy use, and for calculating renewable energy utilization, this resulted in a set of 270 typical hourly data weather files. The properties of the building structure are shown in Table 3. The indoor calculation temperature is set to 26 °C, the ventilation rate is 0.6/h, the long-wave emissivity of the envelope structure is 0.9, and the surface absorption rate is 0.7. The ground reflectivity is 0.2, the time step of Apache sim is set to 6 min, and the preprocessing period is 10 days.

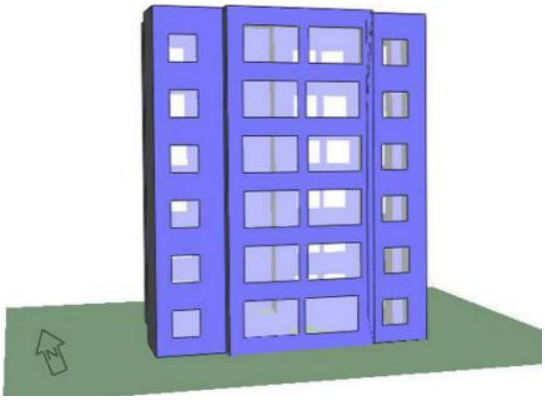

**Figure 2.** Physical model.

**Table 3.** Physical parameters of envelope (GB50176-2016 [28]).

| Name | Structure Level (From Outside to Inside) (mm) | Thermal Conductivity |
|---|---|---|
| Exterior wall | 10 thick facing brick; 30 thick EPS board; 100 thick reinforced concrete; 10 thick gypsum board | 0.58 |
| Roof | 10 thick stone panels; 5 thick asphalt layers; 150 thick cast concrete; 80 thick fiberglass mats; 100 thick hollow blocks; 10 thick ceiling slabs | 0.38 |
| Ground | 25 thick laminated board; 60 thick foam polystyrene insulation board; 100 thick reinforced concrete; 250 thick facing brick; 750 thick clay; | 0.24 |
| Floor | 60 mm paving tiles; 120 mm concrete floor slabs | 2.80 |
| External window (with frame) | Low-e hollow double window | 2.16 |
| Exterior doors | Wooden door | 2.19 |
| Partition | 13 thick cement mortar; 105 thick non-load-bearing hollow brick; 13 thick cement mortar | 1.69 |

## 3. Calculation Results

### *3.1. Building Long-Wave Radiation*

Building long-wave radiation includes the long-wave radiation difference between the horizontal roof and the atmosphere, and the long-wave radiation exchange between the vertical surface of the envelope and the surrounding environment of the building. In response to the impact of different underlying surfaces on the radiation field in open spaces, as well as the effects of architectural enclosed spaces on direct, scattered, and reflected radiation, the simulation software provides varying feedback parameters that require simplification. The building is set as an ideal environment to ignore the long-wave radiation and long-wave reflection of the surrounding building environment. The total summer long-wave radiation of the same building in different climatic regions is calculated by Formula (2), as shown in Figure 3 and Table 4.

Using computational models to calculate the summer long-wave radiation for each city, the results of long-wave radiation range from 442 to 2129 kW and the cooling of summer long-wave radiation is significantly affected by climate. Among them, the summer long-wave radiation in Turpan is as high as 2129 kW, and most cities' long-wave radiation is concentrated at 1479–1782 kW. The cooling effect of long-wave radiation is obviously lower than that of other regions, with the total value in summer of 442 kW and 966 kW, respectively. From the perspective of cooling demand level, the trend of urban long-wave radiation does not have a high correlation with air-conditioning degree days. Except for the relatively stable radiation value in the three-level area, there is a big difference in the

radiation amount of the selected cities at the 1st and 2nd level. It can be seen that the scope of application of long-wave radiation cooling technology is affected by the specific heating factors in each region, and the comprehensive evaluation of the applicability of long-wave radiation cooling technology should be based on the relationship between key meteorological factors in each region and building heat dissipation.

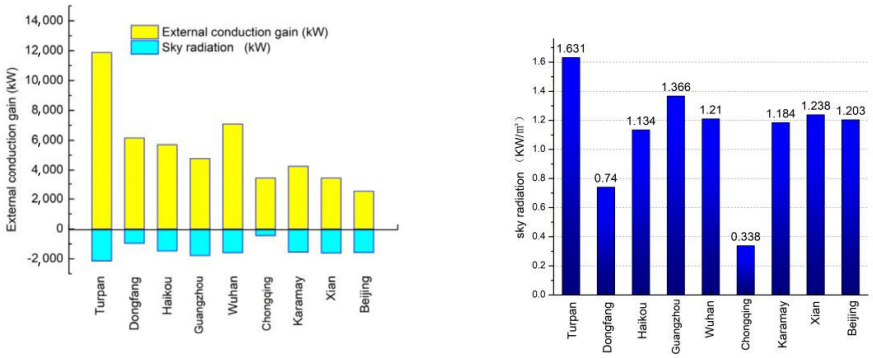


(**a**) External conduction gain (**b**) Sky radiation

**Figure 3.** Long-wave radiation values in summer in each city.

**Table 4.** Load and heat gain data sheet.

| City | Load Difference | Minimum Value | Maximum Value | Gain Ratio | Gain Difference | Gain Minimum | Gain Maximum |
|---|---|---|---|---|---|---|---|
| **Turpan** | 2126.398 | 30,962.782 | 33,089.18 | 0.15201 | 2129 | 11,875.7 | 14,004.495 |
| **Dongfang** | 965.42893 | 18,801.574 | 19,767.00293 | 0.13576 | 966 | 6147.436 | 7113.118 |
| **Haikou** | 1470.00077 | 17,145.29923 | 18,615.3 | 0.20578 | 1479 | 5709.78 | 7189.195 |
| **Guangzhou** | 1755.03814 | 14,635.725 | 16,390.76314 | 0.27186 | 1782 | 4773.4 | 6555.64 |
| **Wuhan** | 1506.636 | 19,471.69 | 20,978.326 | 0.18212 | 1579 | 7092.877 | 8672.26 |
| **Chongqing** | 401.63973 | 12,751.296 | 13,152.93573 | 0.11468 | 442 | 3409.866 | 3851.566 |
| **Karamay** | 1455.25 | 14,635.671 | 16,090.921 | 0.26655 | 1545 | 4252.073 | 5797.382 |
| **Xi'an** | 1501.984 | 11,889.37 | 13,391.354 | 0.32163 | 1616 | 3408.616 | 5024.692 |
| **Beijing** | 1493.81 | 9313.584 | 10,807.394 | 0.38408 | 1570 | 2518.46 | 4088.958 |

### *3.2. Influence of Long-Wave Radiation Heat Transfer*

The heat gain calculation of the outer envelope is the basis of the building load and the thermal design of the envelope. The heat balance of the outer envelope is a comprehensive process of solar radiation heat gain, indoor and outdoor temperature difference heat transfer, and long-wave radiation heat dissipation. In order to explore the actual effect of long-wave radiation on the summer heat gain of the building envelope in different climates, the heat gain influence rate of buildings in each city is calculated:

$$P = \frac{q_l}{q_h + q_l} \cdot 100\% \quad (10)$$

where P is the influence rate of long-wave radiation on building heat gain; $q_l$ is long-wave radiation heat dissipation, kW; and $q_h$ is the heat gain of the building envelope, kW. Figure 4 shows the heat gain and impact rate of the urban envelope structure.

It can be seen from Figure 4 that the variation range of the long-wave radiation influence rate is between 11.4% and 38.4%, and the variation trend is different from the total long-wave radiation value. The long-wave radiation performance and the heat gain of the building itself have a higher influence rate in Beijing and Xi'an, reaching 38.4% and 32.2%. In this area, only one-third of the natural heat gain of the building in summer can be reduced by cooling by long-wave radiation. Under the influence of a low total value of long-wave radiation, the heat gain rate of Chongqing and the Eastern region is lowest,

which is 11.5% and 13.6%, respectively. It is worth noting that the total long-wave radiation in Turpan is much higher than that in other regions, but the impact rate is only 15.2%. This is because the buildings in the Turpan area receive a lot of heat in their natural state, and the heat-proof design of buildings should be integrated with building shading, reflected radiation, and long-wave radiation in this area. In the process of building heat protection design, the long-wave radiation can be determined in different climatic regions according to the building heat gain influence rate, and the outdoor calculation boundary correction can be performed for the areas with high influence rate.

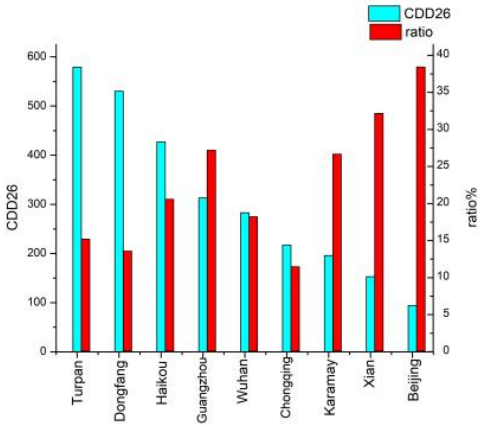


**Figure 4.** Sky radiation cooling ratio.

### *3.3. Applicable Weather Conditions*

It can be seen from Formulas (8) and (9) that the effective sky temperature and ground radiation are the dynamic change process under the combined action of various factors such as absolute air temperature, water vapor partial pressure, hourly insolation rate, and ground albedo. There are many influencing parameters and the calculation process is complicated, so it is difficult to determine the applicability of long-wave radiation technology. Generally, dry bulb temperature, relative humidity, and solar radiation are used as the main meteorological indicators for building load and thermal design in the outdoor environment design of buildings. Therefore, based on the analysis of the calculation results of long-wave radiation cooling, the Turpan area is regarded as the representative area of the high-efficiency application of long-wave radiation cooling technology (ZONE I), Chongqing and the Eastern region are taken as the representative regions of low efficiency in long-wave radiation cooling technology (ZONE III), and other areas are general application areas (ZONE II). By comparing the key meteorological characteristics of the regions represented by the above three types of sky radiation efficiency, the applicable climate range of the sky radiative cooling technology is calculated, as shown in Figures 5–7.

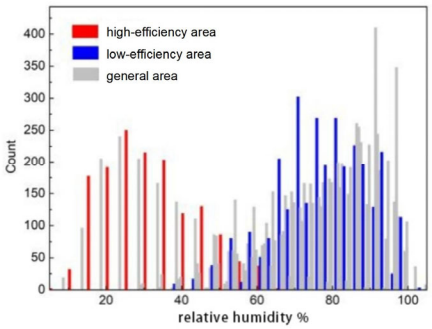


**Figure 5.** Frequency distribution of hourly relative humidity in summer.

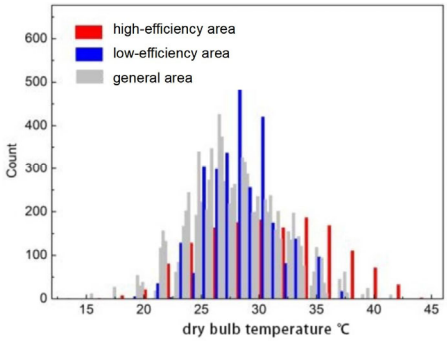


**Figure 6.** Frequency distribution of hourly dry bulb temperature in summer.

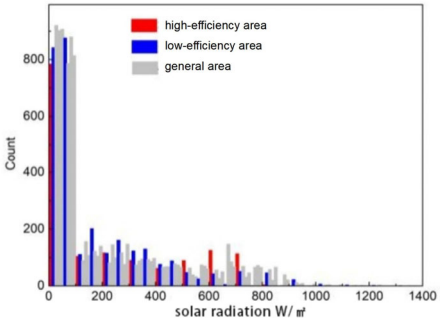


**Figure 7.** Distribution of hourly solar radiation frequency in summer.

It can be seen from Figure 5 that the difference in application caused by the relative humidity index is very significant. The relative humidity range of ZONE I is 10–60%, and the heat dissipation effect of ZONE II is poor at 40–100%. The relative humidity in summer is lower, which is more conducive to long-wave radiation cooling (Figure 8).

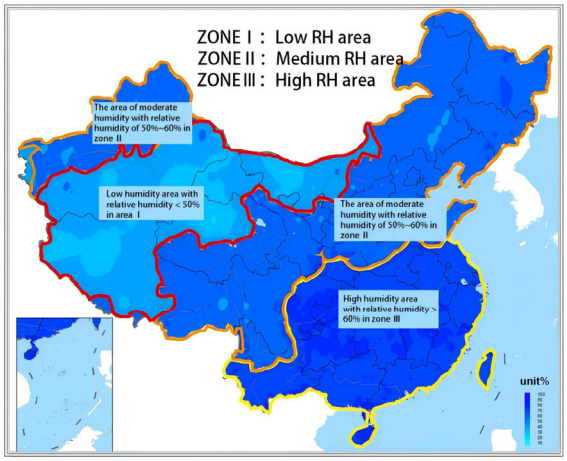


**Figure 8.** Scope of application diagram.

The characteristic maximum temperature of ZONE I is greater than 35 °C, and the distribution of ZONE II has no significant characteristics. The characteristic dry bulb temperature of ZONE III is concentrated at 25–30 °C, and the frequency is higher than 200 h. The larger the mean absolute deviation of the dry bulb temperature, the more favorable it is to radiative cooling of the sky.

The solar radiation ZONE I is uniformly distributed, and the ZONE II distribution has no significant characteristics. The frequency of the characteristic solar radiation of ZONE III decreases in the range of 200–600 W/m$^2$, and the frequency difference between

ZONEs is less than 100. It is not effective to use solar radiation as the evaluation index of sky radiation potential.

## 4. Conclusions

Climate differences significantly affect the cooling effect of long-wave radiation. In the nine typical cities, the long-wave radiation range in summer is 442–2129 kW. Except for a few cities, the long-wave radiation has little difference in the range of 1479–1782 kW, and that in the Turpan area is significantly higher than those in the other areas, with a long-wave radiation value as high as 2129 kW. The long-wave radiation values in the East and Chongqing areas are relatively low, 966 kW and 442 kW, respectively.

A climate feature classification method for long-wave radiation cooling design is proposed, utilizing outdoor relative humidity, dry bulb temperature, and sky effective temperature as crucial indicators to classify the applicable climate. Through the statistical analysis of the hourly frequency, the appropriate climate characteristics of the long-wave radiation cooling technology are obtained as follows: the relative humidity is less than 60% and the outdoor temperature difference is greater than 12 °C.

Long-wave radiation cooling technology can reduce the heat gain of building envelopes in nine selected areas, among which Beijing and Xi'an are more suitable, reaching 38.4% and 32.2%, reducing the natural heat gain of buildings in summer by one-third. In practical applications, the differences in passive heat gain paths of the enclosure structure should be reasonably considered, and technologies such as shading and reflected radiation should be used to help the utilization of long-wave radiation cooling technology.

The analysis of crucial meteorological characteristics across the three types of sky radiation efficiency zones (ZONE I, ZONE II, and ZONE III) reveals the applicable climate range for sky radiative cooling technology; ZONE I's humidity range of 10–60% and higher maximum temperatures (>35 °C) favor long-wave radiation cooling, while ZONE II's higher humidity levels (40–100%) hinder heat dissipation. ZONE III's dry bulb temperature range (25–30 °C) over 200 h indicates a positive correlation between temperature deviations and sky radiative cooling potential.

**Author Contributions:** Conceptualization, J.C.; Software, F.X. and X.J.; Project administration, S.S.Y.L.; Funding acquisition, Y.F. All authors have read and agreed to the published version of the manuscript.

**Funding:** This research was funded by the National Natural Science Foundation of China, grant number no. 52178020, and Guangdong Basic and Applied Basic Research Foundation (no. 2024A1515010891/no. 2023A1515110736).

**Data Availability Statement:** Data will be made available on request.

**Conflicts of Interest:** The authors declare no conflicts of interest.

## References

1. Building Energy Conservation Research Center, Tsinghua University. *China Building Energy Conservation Annual Development Research Report*; China State Construction Industry Press: Beijing, China, 2019; pp. 3–15.
2. Zhao, Z. A Brief Analysis of Building Energy Saving Measures and Renewable Energy Utilization. *Ind. Build.* **2013**, *43*, 94–96.
3. Xie, S.; Chu, D. Thinking and Methods of sustainable Architectural Design. *Ind. Build.* **2019**, *49*, 54–59.
4. Xie, X.; Luo, Z.; Grimmond, S.; Sun, T.; Morrison, W. Impact of inter-building longwave radiative exchanges on building energy performance and indoor overheating. *Build. Environ.* **2022**, *209*, 108628. [CrossRef]
5. Wang, T.; Shi, J.; Ma, Y.; Letu, H.; Li, X. All-sky longwave downward radiation from satellite measurements: General parameterizations based on LST, column water vapor and cloud top temperature. *Isprs J. Photogramm. Remote Sens.* **2020**, *161*, 52–60. [CrossRef]
6. Li, D.; Wang, T.; Zheng, X.; Zhang, P.; Zheng, L.; Leng, W.; Du, Y.; Chen, L.; Zhang, W. Multi-Dimensional matrix MAPping (MDMAP): A new algorithm framework to derive top-of-atmosphere outgoing longwave radiation from space. *Remote Sens. Environ.* **2024**, *304*, 114031. [CrossRef]
7. Xu, J.; Liang, S.; Ma, H.; He, T.; Zhang, Y.; Zhang, G. A daily 5-km all-sky sea-surface longwave radiation product based on statistically modified deep neural network and spatiotemporal analysis for 1981–2018. *Remote Sens. Environ.* **2023**, *290*, 113550. [CrossRef]

8. Li, M.; Peterson, H.B.; Coimbra, C.F.M. Radiative cooling resource maps for the contiguous United States. *J. Renew. Sustain. Energy* **2019**, *11*, 036501. [CrossRef]
9. Zhu, Y.; Qian, H.; Yang, R.; Zhao, D. Radiative sky cooling potential maps of China based on atmospheric spectral emissivity. *Sol. Energy* **2021**, *218*, 195–210. [CrossRef]
10. Chen, J.; Lu, L.; Gong, Q. A new study on passive radiative sky cooling resource maps of China. *Energy Convers. Manag.* **2021**, *237*, 114132. [CrossRef]
11. Brunt, D. Notes on radiation in the atmosphere. I. *Q. J. R. Meteorol. Soc.* **1932**, *58*, 389–420. [CrossRef]
12. Brutsaert, W. On a derivable formula for long-wave radiation from clear skies. *Water Resour. Res.* **1975**, *11*, 742–744. [CrossRef]
13. Maghrabi, A.; Clay, R. Nocturnal infrared clear sky temperatures correlated with screen temperatures and GPS-derived PWV in southern Australia. *Energy Convers. Manag.* **2011**, *52*, 2925–2936. [CrossRef]
14. Bilbao, J.; De Miguel, A.H. Estimation of Daylight Downward Longwave Atmospheric Irradiance under Clear-Sky and All-Sky Conditions. *J. Appl. Meteorol. Clim.* **2007**, *46*, 878–889. [CrossRef]
15. Li, M.; Jiang, Y.; Coimbra, C.F.M. On the determination of atmospheric longwave irradiance under all-sky conditions. *Sol. Energy* **2017**, *144*, 40–48. [CrossRef]
16. Chen, Q. *Selected Works of Chen Qigao on Architectural Physics*; China State Construction Industry Press: Beijing, China, 2004; pp. 452–455.
17. Evangelisti, L.; Guattari, C.; Asdrubali, F. On the Sky Temperature Models and Their Influence on Buildings Energy Performance: A Critical Review. *Energy Build.* **2019**, *183*, 607–625. [CrossRef]
18. *ASHRAE Standard 169-2006*; Weather Data for Building Design Standards. American Society of Heating, Refrigerating and Air-Conditioning Engineers: Atlanta, GA, USA, 2006.
19. Prata, A.J. A new long-wave formula for estimating downward clear-sky radiation at the surface. *Quart. J. Roy. Meteorol. Soc.* **1996**, *122*, 1127–1151.
20. Dilley, A.C.; O'Brien, D.M. Estimating downward clear sky long-wave irradiance at the surface from screen temperature and precipitable water. *Quart. J. Roy. Meteorol. Soc.* **1998**, *124*, 1391–1401.
21. Marthews, T.R.; Malhi, Y.; Iwata, H. Calculating downward longwave radiation under clear and cloudy conditions over a tropical lowland forest site: An evaluation of model schemes for hourly data. *Theor. Appl. Clim.* **2011**, *107*, 461–477. [CrossRef]
22. Crawford, T.M.; Duchon, C.E. An improved parameterization for estimating effective atmospheric emissivity for use in calculating daytime downwelling long-wave radiation. *J. Appl. Meteorol.* **1999**, *38*, 474–480. [CrossRef]
23. Konzelmann, T.; Van de Wal, R.S.W.; Greuell, W.; Bintanja, R.; Henneken, E.A.C.; Abe-Ouchi, A. Parameterization of global and longwave incoming radiation for the Greenland Ice Sheet. *Glob. Planet. Chang.* **1994**, *9*, 143–164. [CrossRef]
24. Sridhar, V.; Elliott, R.L. On the development of a simple downwelling long-wave radiation scheme. *Agric. Meteorol.* **2002**, *112*, 237–243. [CrossRef]
25. Iziomon, M.G.; Mayer, H.; Matzarakis, A. Downward atmospheric longwave irradiance under clear and cloudy skies: Measurement and parameterization. *J. Atmos. Sol.-Terr. Phy* **2003**, *65*, 1107–1116. [CrossRef]
26. Duarte, H.F.; Dias, N.L.; Maggiotto, S.R. Assessing daytime downward long-wave radiation estimates for clear and cloudy skies in Southern Brazil. *Agric. Meteorol.* **2006**, *139*, 171–181. [CrossRef]
27. Lhomme, J.P.; Vacher, J.J.; Rocheteau, A. Estimating downward long-wave radiation on the Andean Altiplano. *Agric. For. Meteorol.* **2007**, *145*, 139–148. [CrossRef]
28. *GB 50176-2016*; Code for Thermal Design of Civil Buildings. Ministry of Housing and Urban-Rural Development of the People's Republic of China: Beijing, China, 2016.
29. Zhang, H. *Research on Time Domain Division of Climate Adaptability for Building Energy Efficiency*; Chongqing University: Chongqing, China, 2009.